EVS29 Symposium
Montréal, Québec, Canada, June 19 - 22, 2016

Influence of in-wheel motors weight on a swing-arm dynamic, evaluation of ride comfort and handling

Jean-Sébastien Brest[1*], Yoann Gimbert[1]
[1]*Altran Research, TECHN'HOM 4 - Bâtiment 66.C, 11 rue de la découverte, 90000 Belfort, France,*
[*]*Corresponding author: jean-sebastien.brest@altran.com*

Abstract

This paper presents a model aiming at describing the influence of an additional mass on an urban vehicle. The impact of an in-wheel motor on the road holding performances and vehicle comfortableness, for which criteria have been defined, has been studied on a swingarm and compared to a standard configuration (vertical suspension). Simulations have been carried out using Matlab Simulink and a comparison has been made using several obstacles as well as different types of roads.

Keywords: BEV, Wheel hub motor, Simulation, Modeling

1 Introduction

With the large shift in oil prices and growing concerns about the environmental impact of internal combustion engines, and the political support towards alternative powertrains, electric vehicle have become the solution in many minds. Whether they are fully electric or hybrid, the automobile industry is moving towards e-mobility: this type of vehicle is increasingly present on the roads. This has become a strong sales argument over the years, to the point that hybrid supercars have been developed in the last few years.
Despite the progress made, the performances (particularly in the vehicle's range) and the costs (if states subventions are not considered) of electric vehicles are really an obstacle to the transition from the classical internal combustion engine (ICE). The three best-selling electric cars in France in 2015 don't exceed 250 km of autonomy (announced, in real conditions it is reduced of at least 25% [1]). For hybrid vehicles, the electrical autonomy falls to 50 km, the ICE being privileged.
The in-wheel motor is an interesting technology to power new electric vehicles and meet the growing demands of both electric **and** hybrid vehicles [2]. It provides interesting advantages over conventional electric engines since multiple parts of the transmission are removed:

- consequent weight saving,
- manufacturing costs reduction,
- an improvement of the drive train efficiency,
- freeing up space.

Those gains may allow to increase the battery pack's size, thus the autonomy and reduce the range anxiety [3] for example.
However, this technology implies an increase of the unsprung weight. This additional mass is known to deteriorate the ride comfort and its road handling [4], even if studies have shown that its effect might be negligible [5, 6]. This work presents an analytical study aiming at quantifying the comfort and handling

losses induced by the use of an in-wheel motor, integrated in the rear wheel, mounted on a swingarm. Rather than just focusing on the parameters of a quarter vehicle suspension model [7], we chose to study a 2 dimensions vehicle model (so the pitch and heave motions are considered), and compared the results obtained on a conventional vertical system.

2 Criteria definition

Before presenting the models or the results associated, it is necessary to begin with the definition of the criteria used to define comfort and road holding as well as the definition of the road.

2.1 Comfort definition

Many people spend a significant amount of time in transportation (distances traveled have substantially grown in the past decades), leading in an increasing demand for comfort. For prestige (image of the manufacturer) as well as security reasons (more comfort means less fatigue), the interest in the evaluation of ride comfort is increasing. There are two ways to assess performances in terms of physical comfort: through a subjective method, or using an objective criterion. The first one involves a panel of people to test the vehicle experimentally, and evaluate the comfort through their experience. Unfortunately, to obtain comparable results between several vehicles, the experimenter has to stay the same, and so has his mood. In our case, the evaluation of comfort related to unsprung masses requires an objective criterion. It has to be based on the specific variables that are mostly affected by those masses' variations: the accelerations.
If the human body is sensitive to accelerations, their consequences on comfort will not be the same according to their directions and frequencies. That sensitivity can be described by weighting curves as a function of the frequencies for both the vertical (figure 1 a) and horizontal (figure 1 b) accelerations [8].

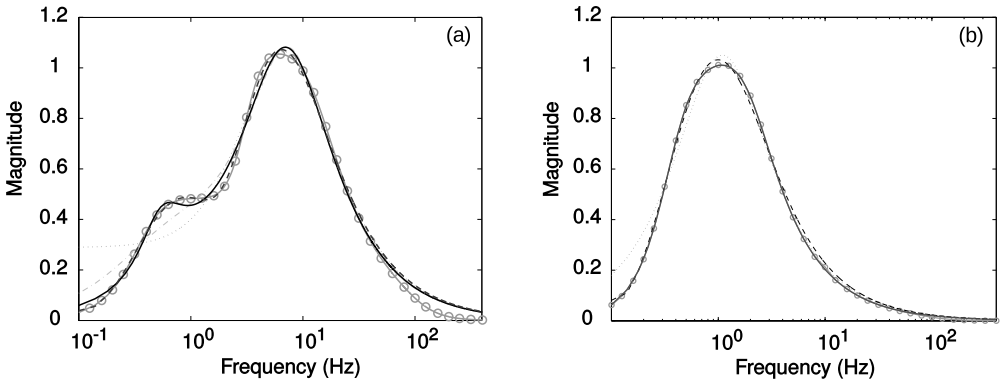

Figure 1: Frequency-weighting curves W_k and W_d - circles respectively on (a) and (b) - and quasi-least-square filter approximations: second order (dot), third order (dash), fourth order (solid), fifth order (dash-dot) [9].

To approximate those curves, Zuo et al. [9] have proposed to use frequential filters so that only the frequencies to which the human body is sensitive would be considered. The equations for those filters are:

$$W_k^{(5)}(s) = \frac{87.72s^4 + 1138s^3 + 11336s^2 + 5453s + 5509}{s^5 + 92.6854s^4 + 2549.83s^3 + 25969s^2 + 81057s + 79783} \quad (1)$$

$$W_d^{(4)}(s) = \frac{12.66s^3 + 163.7s^2 + 60.64s + 12.79}{s^4 + 23.77s^3 + 236.1s^2 + 692.8s + 983.4} \quad (2)$$

where W_k and W_d represent respectively the weighting curves for vertical and horizontal accelerations, and s is the Laplace variable.

Assuming the vehicle ride comfort can be evaluated by the intensity of the accelerations of the sprung body, one can use a ride comfort index (RCI) [10, 11], according to the scale suggested in table 2 [8]: the lower the RCI is, the more comfortable the vehicle is considered to be.
The RCI is obtained by:

$$RCI = \sqrt{\ddot{Z}_{rms}^2 + \ddot{X}_{rms}^2} \quad (3)$$

Table 1: Scale of vibration discomfort [8].

RMS weighted acceleration	Comfort
Less than 0.315 m.s^{-2}	not uncomfortable
0.315 to 0.63 m.s^{-2}	a little uncomfortable
0.5 to 1 m.s^{-2}	fairly uncomfortable
0.8 to 1.6 m.s^{-2}	uncomfortable
1.25 to 2.5 m.s^{-2}	very uncomfortable
Greater than 2.5 m.s^{-2}	extremely uncomfortable

with $\ddot{Z}_{rms}$ and $\ddot{X}_{rms}$ the frequency weighted root mean square values (calculated using the power spectral density of the signal obtained via equations 1 and 2) of the acceleration in the Z and X directions.

2.2 Road holding criterion

Vehicle handling is a broad term that can encompass different parameters such as rolling resistance, adhesion during cornering, braking and acceleration, directional stability... In our study, we have selected road holding as a criterion. We have considered it to be the maximum lateral acceleration admissible by a tire without losing adhesion. In the same way as for the comfort, an objective criterion has to be defined to quantify the road holding of the vehicle.

Tires being the only contact between the car and the road, they have a major impact on the vehicle road holding. In a bend, the lateral forces of the tires are counteracting the centrifugal acceleration of the car. If the lateral forces are not large enough, the vehicle will deviate from its path or even skid and get out of control. Thus, in order to have good road holding, the lateral forces should be maximized. However, the value of these forces is dependent on the vertical load of the tire [12]. Pacejka shows that, when cornering on a rough road, the vertical load of a tire is fluctuating (F_Z on Fig. 2 (c)), and these fluctuations create a loss of the tire side force (F_Y Fig. 2 (a)).

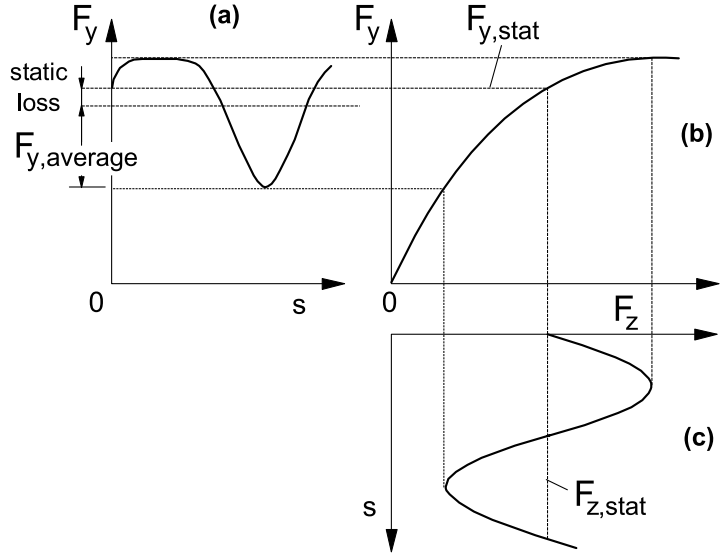

Figure 2: The static loss in average side force due to the curved force vs load relationship [12].

Consequently, the fluctuation of the vertical load of this tire can be used as a road holding criterion: the larger the fluctuations of the side forces are, the larger the losses in cornering power are, and the worse the road holding is. Therefore, the standard deviation, which is a statistical measure of the variation of a set of data, can be used to quantify the fluctuation of the vertical load and can be considered as a road holding index.

2.3 Road modelling

Those two criteria can only be valid or efficient if the road or the obstacles to cross are properly modeled. Two main situations have been considered in this study: driving over an obstacle and driving on a road of given roughness. The first one corresponds to a speed bump [7], a speed cushion or a sidewalk step, modeled by a more or less abrupt climb (Fig. 3) at limited speed (around 30 km.h^{-1}).

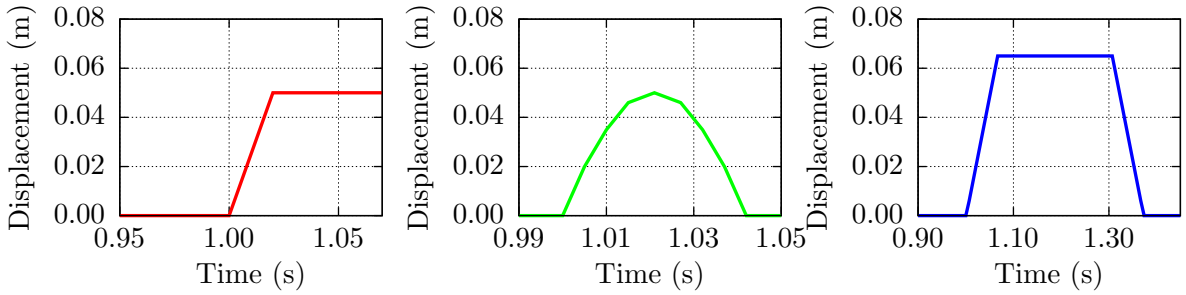

Figure 3: Imposed displacements on the wheel representing a sidewalk step (left), a speed bump (middle) and a speed cushion (right).

For the second situation, the work of Tyan et al. [13] is used in order to generate random road profiles of given roughness. According to [14], the roughness of a portion of road can be characterized by its degree of roughness (Tab. 2).

Table 2: Classification of road roughness [14].

Road class	quality	Degree of roughness $\Phi(\Omega_0)$ (10^{-6}m^2/(cycle/m))
A	Very good	< 8
B	Good	8-32
C	Average	32-128
D	Poor	128-512
E	Very poor	> 512

The profile of a random road can be described using the following standard formulation of the power spectral density of the surface profile $\Phi(\Omega)$ [14]:

$$\Phi(\Omega) = \begin{cases} \Phi(\Omega_0) \cdot \Omega_1^{-w}, & \text{for } 0 < \Omega < \Omega_1 \\ \Phi(\Omega_0) \cdot \left(\frac{\Omega}{\Omega_0}^{-w}\right), & \text{for } \Omega_1 < \Omega < \Omega_n \\ 0, & \text{for } \Omega_n < \Omega \end{cases} \quad (4)$$

where $\Omega = \frac{2 \cdot \pi}{\lambda}$ is the angular spatial frequency, λ is the wavelength and Ω_0 (rad.m^{-1}) is the reference wave number, w the waviness.
In order to generate a random road, Tyan et al. give the expression of the road height in the time domain:

$$z_0(t) = \sum_{n=1}^{N} A_n \cdot \sin(n \cdot \omega_0 \cdot t - \phi_n) \quad (5)$$

with $A_n = \sqrt{\Phi(\Omega_n) \cdot \frac{\Delta\Omega}{\pi}}$ the amplitudes and $\Phi(\Omega_n)$ obtained in eq. 4. $\Delta\Omega = \frac{2\pi}{L_r}$ is the frequency step, N represents the number of harmonics, $\omega_0 = v \cdot \Delta\Omega$ is the fundamental temporal frequency and ϕ_n the phases angles treated as a random variable following a uniform distribution in the interval $[0, 2\pi]$. This expression can then be easily used to generate road profiles in Matlab through the sum of different sine waves.

3 Vehicle modelling

The purpose of the study is to evaluate the impact of an in-wheel motor on an urban vehicle which would be equipped with an oscillating arm, more specifically, on a three-wheeler with two front wheels and the swingarm for the rear wheel. In the interest of simplification, the model represents a 2 dimensions vehicle (Figure 4). For the front wheel, a simple two degrees of freedom system is used, the rear part of the vehicle is modelled by a swingarm. The comparison of the results obtained with this model will be compared to the ones obtained with a model composed of a simple two degrees of freedom system for the rear wheel.

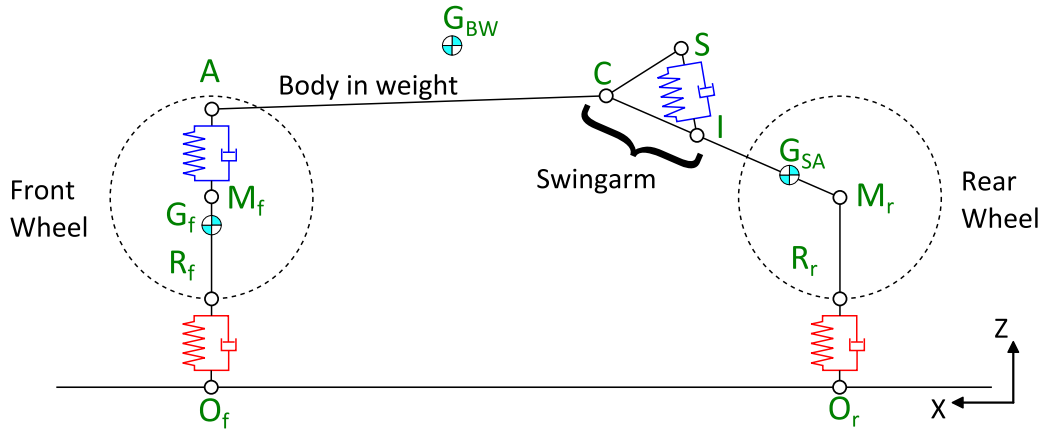

Figure 4: Schematic representing the model used in this study.

Such a configuration allows taking into account the pitch and heave motions. Furthermore, the wheel-hop phenomenon, corresponding to the loss of contact between the road and the tire, was incorporated in the model.
Some assumptions have been made in this study, the vehicle aerodynamic effect is neglected the vehicle is assumed to be rigid so the load transfer from one point to another is loss less. Parameters of the vehicle are also assumed to be constant (such as tire stiffness, spring stiffness, damper coefficient...) throughout the two models to allow comparison.

The expression of the force, F_{ft}, due to the tire spring and damper on the front wheel is written:

$$F_{ft} = \begin{cases} \left[\left(Z_{R_f} - Z_{O_f}\right) - L_{ft}^0\right] K_{ft} + \left[\dot{Z}_{R_f} - \dot{Z}_{O_f}\right] C_{ft}, & \text{for } Z_{R_f} - Z_{O_f} \leq L_{ft} \\ 0, & \text{for } Z_{R_f} - Z_{O_f} \geq L_{ft} \end{cases} \tag{6}$$

Z_{O_f} is the height of the road at the contact point O_f of the front tire, Z_{R_f} is the height of the point R_f, and L_{ft} is the initial length of the spring equivalent to the tire. K_{ft} and C_{ft} are respectively the stiffness and the damping coefficient of the front tire. The force is considered null when the contact between the road and the tire is lost. The expression for the rear wheel is the same, the index f (standing for forward) being replaced by r (standing for rear).
The force related to the front suspension F_{fs} is:

$$F_{fs} = \left[\left(Z_A - Z_{R_f} - Z_{ts}\right) - L_{fs}^0\right] K_{fs} + \left[\dot{Z}_A - \dot{Z}_{R_f}\right] C_{fs} \tag{7}$$

Where Z_A is the height of the point A, Z_{ts} is the distance between the tire's spring and the suspension and L_{fs} is the initial length of the front suspension. K_{fs} and C_{fs} are respectively the stiffness and the damping coefficient of the front suspension.
The force due to the rear suspension F_{rs} (for the swingarm) is:

$$F_{rs} = \left[L_{rs} - L_{rs}^0\right] K_{rs} + \dot{L}_{rs}(t) \cdot C_{rs} \tag{8}$$

with L_{rs} the length of the rear suspension and L_{rs}^0 its initial value. K_{rs} and C_{rs} are respectively the rear suspension stiffness and damping coefficient.

The model is composed of three bodies, the front wheel, the swingarm (including the rear wheel) and the body in weight (corresponding to sprung masses). Newton's second law was applied to each one of them. For the front wheel in the Z direction:

$$m_f \cdot \ddot{Z}_A = -m_f \cdot g + F_{fs} - F_{ft} \tag{9}$$

With m_f the mass of the front wheel and g the acceleration of gravity. For the swingarm in the Z direction:

$$m_r \cdot \ddot{Z}_{G_{SA}} = -m_r \cdot g - F_{rt} + F_{rs} \cdot \cos\theta_S + F_{rZ} \tag{10}$$

With m_r the mass of the swingarm and the rear wheel, $Z_{G_{SA}}$ the height of their center of gravity G_{SA}. θ_S is the angle between the rear suspension (point C to point M_r) and the Z axis, and F_{rZ} is the force applied by the swingarm and the rear wheel on the car body at the point C in the Z direction. For the swingarm in the X direction:

$$m_r \cdot \ddot{X}_{G_{SA}} = F_{rs} \cdot \sin + \theta_S F_{rX} \tag{11}$$

With $X_{G_{SA}}$ the swingarm and rear wheel's center of gravity position in the axis X direction, and F_{rX} is the force applied by the swingarm and the rear wheel on the car body at the point C in the X direction. For the swingarm, around the Y axis, applied on G_{SA}:

$$I^y_{G_{SA}} \ddot{\theta}_{SA} = -M\left(F_{rt}\right)^{G_{SA}} - M\left(F_{rZ}\right)^{G_{SA}} + M\left(F_{rX}\right)^{G_{SA}} - M\left(F_{rs}\right)^{G_{SA}} \tag{12}$$

With $I^y_{G_{SA}}$ the moment of inertia of the swingarm around the Y axis applied on G_{SA}. $\theta_{SA} = \frac{\pi}{2} - \theta_S$ is the angle between the swingarm and the X axis. $M(F)^P$ stands for the moment of the force F around the Y axis, applied on the point P. For the car body in the Z direction:

$$m_{BW} \cdot \ddot{Z}_{G_{BW}} = -F_{rX} - F_{rs} \cdot \cos(\theta_S) - F_{fs} - m \cdot g \tag{13}$$

For the car body around the Y axis at the point G_{BW}:

$$I^y_{G_{BW}} \ddot{\theta}_C = 2M\left(F_{fs}\right)^{G_{BW}} + M\left(F_{rX}\right)^{G_{BW}} - M\left(F_{rX}\right)^{G_{BW}} - M\left(F_{rs}\right)^{G_{BW}} \tag{14}$$

With θ_C the angle between the body in weight and the swingarm.

4 Results

The simulation parameters of the results presented in this paper are shown in Table 3. The results are structured in two categories, the first one aims at studying the impact of speed on the two indexes described above, on a classic configuration and on an swingarm. The second one focuses on the influence of unsprung to sprung ratio on the model equipped with an swingarm.

Table 3: Model parameters

Symbol	Value	Symbol	Value
m_{tot}	700 kg	m_{OA}	15 kg
g	9.81 m.s^{-2}	K_{ft}	150000 N.m^{-1}
K_{rt}	150000 N.m^{-1}	K_{fs}	$4 \cdot \pi^2 \cdot m_{tot}$ N.m^{-1} []
K_{rs}	$4 \cdot \pi^2 \cdot m_{tot}$ N.m^{-1} []	C_{ft}	50 N.m^{-1}
C_{rt}	50 N.m^{-1}	C_{fs}	$\pi^2 \cdot m_{tot}$ N.m^{-1} []
C_{rs}	$\pi^2 \cdot m_{tot}$ N.m^{-1} []	L_{ft}	0.1 m
L_{rt}	0.1 m	L_{fs}	0.4 m
L_{rs}	0.4 m	X_{AC}	1.3 m
Z_{AC}	0.1 m	X_{CM_r}	0.5 m
Z_{CM_r}	0.3 m	X_{CI}	0.3 m
X_{CS}	0.3 m	Z_{AS}	0.2 m
$I^Y_{G_{BW}}$	220 kg.m^2	$I^Y_{G_{BW}}$	220 kg.m^2
$X_{AG_{BW}}$	0.7 m	$Z_{AG_{BW}}$	0.35 m
X_{AG_f}	0.3 m	Z_{AG_f}	0.2 m
$L_{CG_{OA}}$	$0.5 \cdot L_{CM_r}$		

4.1 Classic configuration vs. swingarm

This part is dedicated to the comparison of the influence of the comfort and road holding indexes between a conventional configuration (simple two degrees of freedom system for both wheels) and the model presented above with an swingarm. The results are presented in Figure 5 for speeds ranging from 30 to 120 km.h^{-1} on roads of class A, C and E.

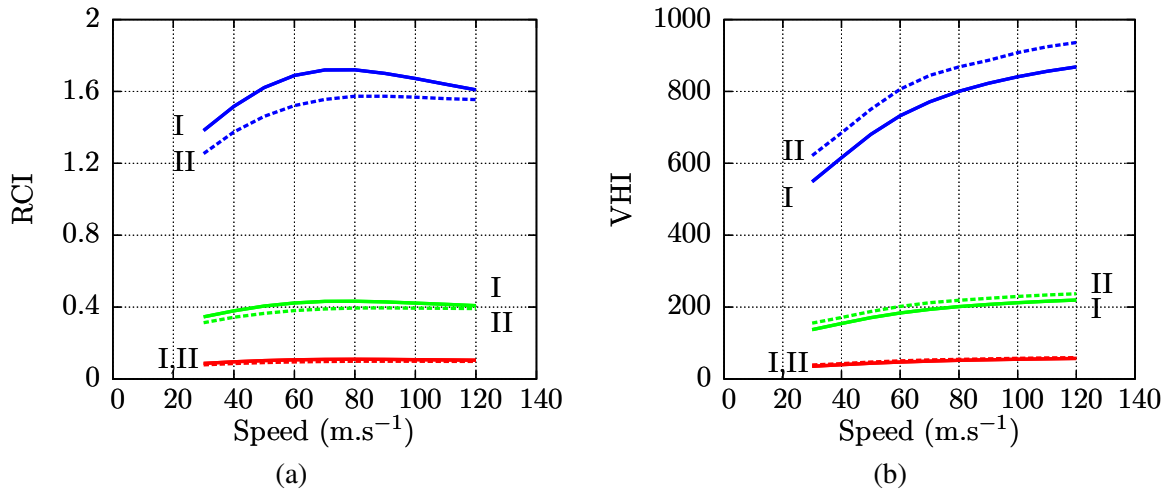

Figure 5: Evolution of the Ride Comfort Index (a) and the Vehicle Handling Index (b) according to speed, for the classical (I - solid lines) and swingarm (II - dashed lines) models on a class A (red - bottom), C (green - middle) and E (blue - top) road.

The RCI is reduced with the use of an swingarm in comparison with a classical configuration. For the first one, the index grows until a limit speed of 75 km.h^{-1} when it starts to slowly decrease. For the other model, we have a similar behaviour with a speed limit of 85 km.h^{-1} and a more important drop after this speed. The evolutions for the two models appear to be quite similar for the VHI, with a handling index slightly higher with the swingarm. Contrary to the RCI, this index is steadily increasing with speed. A lower index being better, the swing arm brings more comfort but degrade vehicle handling.

To evaluate the impact of speed on the two configurations separately, the relative evolution of the two indexes for the class A road are plotted in Figure 6. The values obtained at 30 km.h^{-1} are used as references. The evolutions for the other classes were similar to those ones, and thus are not represented.

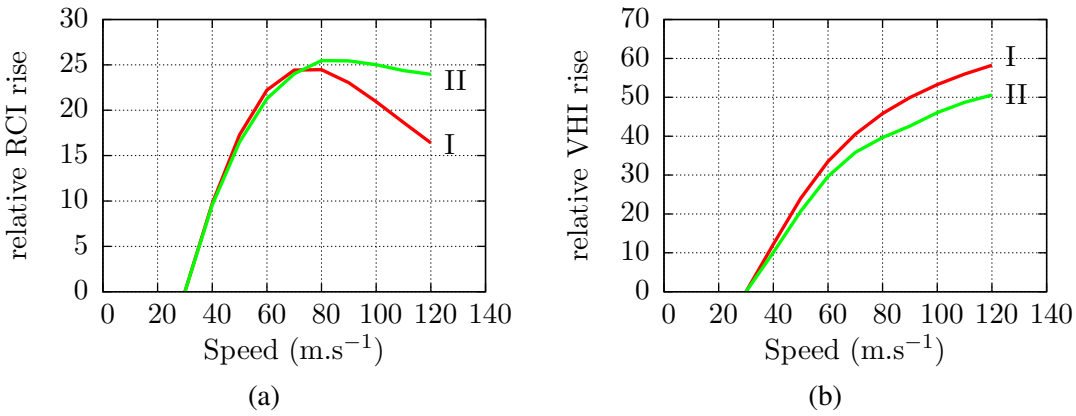

Figure 6: Relative evolution of the RCI (a) and VHI (b) on a class A road, on the classical (red - I) and swingarm (green - II) models.

The configurations studied here show that the evolution of comfort index is similar for speeds lower than 70 km.h^{-1}. Above that limit, for the classical configuration, the RCI falls of 8% for the classical configuration when the presence of the swingarm leads to a less significant loss (2%). The latter appears

to reduce the comfort for high speeds. On the contrary, the consequence of the swingarm on the VHI is a reduction of the index. This time its impact on the results is more positive.

4.2 Influence of the unsprung to sprung masses ratio

This time the attention is focused on the influence of the unsprung to sprung masses ratio. In order to study the influence of the rear wheel unsprung mass on the two above-mentioned indexes, the unsprung to sprung mass ratio is increased with a constant vehicle mass, by a transfer from the sprung to unsprung masses. It corresponds to the study of a conventional motorized vehicle (with the motor is in the sprung mass) changed to an in-wheel motor vehicle.
The Figure 7 is a plot of the indexes according to this ratio for the two studied configurations.

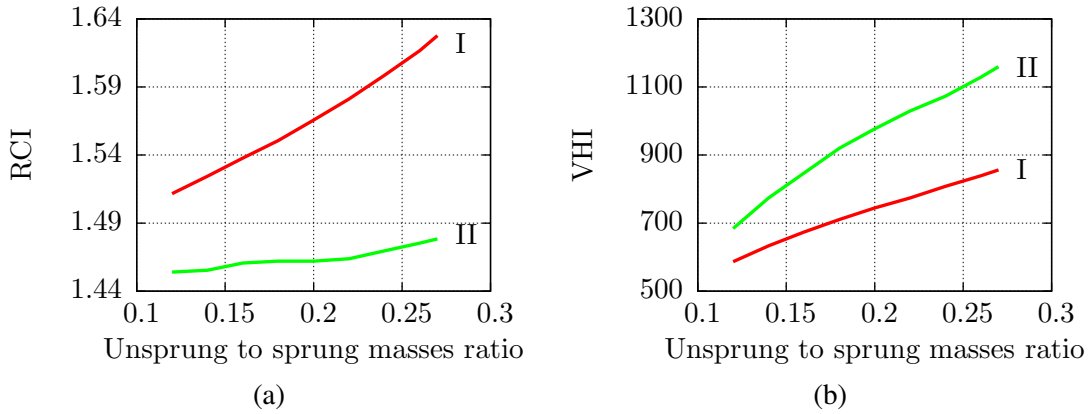

Figure 7: Evolution of RCI (a) and VHI (b) for several unsprung over sprung masses ratio, on a class E road, on the classical (red - I) and swingarm (green - II) models.

It is interesting to notice that the RCI increase is less marked with the swingarm, 1.7% in total against 7.7% for the conventional configuration. It means that the swingarm is not very sensitive to the evolution of the unsprung masses in terms of comfort. For the VHI evolution, for both configurations, more unsprung masses leads to an increase, of 70% with the swingarm and 46% with the classical configuration.

The results obtained for the crossing of common obstacles at a speed of 30 km.h^{-1} are plotted in Figure 8. Once again, the impact of the swingarm on the comfort index is small, except for the speed cushion that shows an increase until stabilization for a 0.2 ratio. One can notice that crossing the latter has also a more important effect on the RCI.

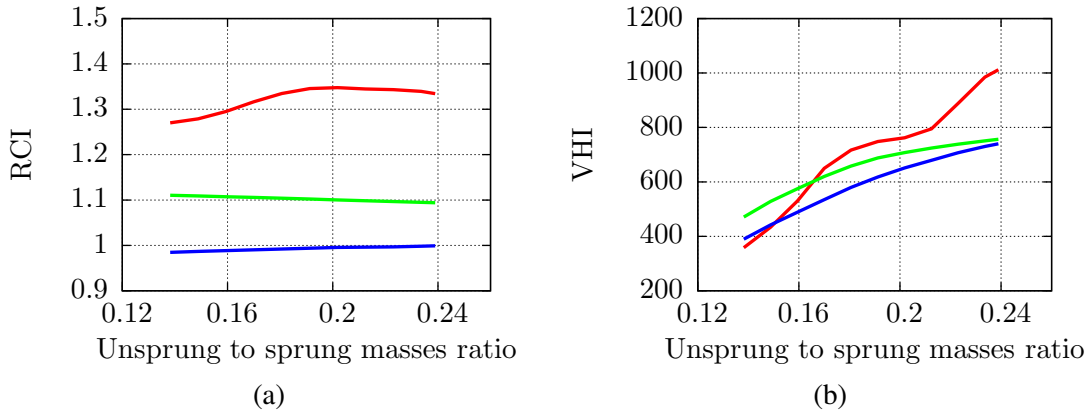

Figure 8: Evolution of RCI (a) and VHI (b) for several unsprung over sprung masses ratio, sidewalk step (blue), a speed bump (green) and a speed cushion (red), on the swingarm model.

5 Conclusion

In this paper, a vehicle model including a swingarm has been studied. This model was constructed in Matlab Simulink. Criteria of comfort and road holding have been defined in order to quantify the impact on the passengers' sensations and the vehicle's behaviour. The results obtained with this model were compared to the ones obtained with a conventional half car model (vertical suspensions). The influence of the unsprung to sprung masses ratio has also been studied. The simulations were performed on different profiles of roads (defined by their roughness) as well as on different obstacles.

The first results presented have shown that the swingarm will basically increase the comfort at the expense of vehicle handling. At low speeds, the evolution of both indexes are similar for both models. For higher speeds, the evolution of comfort is better with the conventional model, and slightly worse with the vehicle handling.
The results obtained have also underlined that the swingarm configuration is less sensitive in terms of comfort to the variation of the unsprung to sprung masses ratio. Less markedly, the evolution of vehicle handling is more affected by the increase of this ratio. The observations made on the different obstacles show the same trend. On this bases, the optimization of both suspension parameters and geometrical configuration could compensate the unsprung mass increase more efficiently than with a conventional vehicle configuration.

References

[1] J.-S. Brest and L. Boulat, "Development of a representative cycle for electric vehicle energy assessment," in *Proceedings of the European Battery, Hybrid and Fuel Cell Electric Vehicle Congress (EEVC-2015)*, 2015.

[2] K. Donghyun, S. Kyeongho, K. Youngkwang, and C. JAESEUNG, "Integrated design of in-wheel motor system on rear wheels for small electric vehicle," *World Electric Vehicle Journal*, vol. 4, 2010.

[3] M. Nilsson, "Electric Vehicle: The phenomenon of range anxiety," tech. rep.

[4] M. Guiggiani, *The Science of Vehicle Dynamics*. Springer Netherlands, 2014.

[5] M. Anderson and D. Harty, "Unsprung mass with in-wheel motors-myths and realities," *AVEC 2010*, pp. 261–266, 2010.

[6] J. Cuadrado, D. Vilela, I. Iglesias, A. Martín, and A. Peña, "A multibody model to assess the effect of automotive motor in-wheel configuration on vehicle stability and comfort," in *ECCOMAS Multibody Dynamics*, 2013.

[7] T. Rao, R. Mohan, G. V. Rao, K. S. Rao, and A. Purushottam, "Analysis of passive and semi active controlled suspension systems for ride comfort in an omnibus passing over a speed bump," *International Journal of Research and Reviews in Applied Sciences*, vol. 5, no. 1, 2010.

[8] I. O. for Standardization, "Mechanical vibration and showk - evaluation of human exposure to whole body vibration - part 1: general requirements," vol. ISO 2631-1:1997, 1997.

[9] L. Zuo and S. A. Nayfeh, "Low order continuous-time filters for approximation of the iso 2631-1 human vibration sensitivity weightings," *Journal of Sound and Vibration*, vol. 265, no. 2, pp. 459–465, 2003.

[10] M. J. Griffin, "Discomfort from feeling vehicle vibration," *Vehicle System Dynamics*, vol. 45, pp. 679–698, July 2007.

[11] R. Vos, I. Besselink, and H. Nijmeijer, "Influence of in-wheel motors on the ride comfort of electric vehicles," in *Proceeding of the 10th International Symposium on Advanced Vehicle Control (AVEC'10)*, pp. 835–840, 2010.

[12] H. Pacejka, *Tire and Vehicle Dynamics, Third Edition*. Butterworth-Heinemann, Apr. 2012.

[13] Y.-F. H. Feng Tyan, "Generation of random road profiles," *J. Advanced Eng.*, vol. 4, 2009.

[14] I. O. for Standardization, "Mechanical vibration - road surface profiles - reporting of measured data," vol. ISO 8608:1995, 1995.

Authors

Jean-Sébastien Brest received a Ph.D. in Mechanical Engineering in 2014 from the University of South Brittany. Currently, he works in Altran's internal Research department in France. He is in charge of two projects related to the automotive industry, a three wheeled experimental platform called V3R (object of the paper) and a consumption simulator called SAGES.

Yoann Gimbert received a Diplôme d'Ingénieur (M.Sc. in General Engineering) from Ecole Centrale Lyon in 2016. He worked in the Research department of the consultancy group Altran during his final year internship. He worked on an innovative three-wheeled vehicle project and his research interest was vehicle dynamics. He is currently working as a mechanical engineer in the automotive area.